

# A giant Ly $\alpha$ cloud associated with a dust-lane radio galaxy at $z = 2.468$ \*

Gopal-Krishna<sup>1,2</sup> \*\*, E. Giraud<sup>1</sup> \*\*\*, J. Melnick<sup>1</sup>, and M. della Valle<sup>1</sup> †

<sup>1</sup> European Southern Observatory, Casilla 19001, Santiago, 19, Chile

<sup>2</sup> Max-Planck-Institut f. Radioastronomie, Postfach 2024, D-53010 Bonn, Germany

Received 27 December 1994 / Accepted 12 April 1995

**Abstract.** We report the discovery of a giant cloud of Ly $\alpha$  emission ( $z = 2.468$ ) associated with an ultra-steep spectrum radio galaxy. The cloud is seen to be confined between the nucleus and the southern hot spot of the double radio source. Its morphology provides evidence for a disk of dusty material around the parent optical galaxy, which probably obscures any Ly $\alpha$  emission that may be associated with the far side of the radio galaxy. The proposal that the observed cloud is spatially coincident with the radio lobe approaching us is substantiated by the measured velocity gradient across the cloud. Further, an analogous situation is shown to exist in some other high- $z$  radio galaxies where the Ly $\alpha$  emission exhibits similarly a large asymmetry about the radio nucleus. Circum-galactic dusty disks may, thus, be a fairly common feature of high- $z$  radio galaxies.

The (tilted) Ly $\alpha$  line of the present object has an extremely large equivalent width ( $\sim 1000$  Å in the rest frame) and is found to be clearly split into two velocity components. The kinematical interpretation of this result is that the nebula is expanding at a velocity of  $\approx 550$  km s<sup>-1</sup> driven by the radio lobe it surrounds. Our data thus provides a kinematical estimate for the age of the radio source of  $\approx 2 \times 10^7$  yrs.

**Key words:** galaxies: active – galaxies: redshifts – radio continuum: galaxies – galaxies: evolution – galaxies: OTL 0852+124

## 1. Introduction

Although Ly $\alpha$  emission is now known to dominate the UV spectra of most high- $z$  radio galaxies, it is found in a few cases to arise from enormously extended clouds ( $\sim 100$  kpc) showing

\* Based on observations made at the European Southern Observatory and with the VLA. The VLA is operated by Associated Universities Inc. under Cooperative Agreement with the National Science Foundation.

\*\* Permanent address: National Centre for Radio Astrophysics, Tata Institute of Fundamental Research, Poona Univ. Campus, Pune-411007, India

\*\*\* Permanent address: Observatoire de Marseille, Place Le Verrier, 13 248 Marseille Cedex 4, France

† Present Address: Dipartimento di Astronomia, Università di Padova, Italy

large and highly turbulent velocity fields ( $\sim 10^3$  km s<sup>-1</sup>), often low-excitation spectra, and an intriguing lack of any bright continuum feature that would signify a well condensed host galaxy (Spinrad 1989). Such remarkable, though rare objects with spectral signatures of nearly pure hydrogen nebulae are often perceived to be ‘forming galaxies’, or ‘immature galaxies in formation’, where the main body of stars is still unborn and, yet, the core has already developed a supermassive central engine capable of producing an extremely powerful double radio source (Spinrad 1987; McCarthy et al. 1987). Such objects, without known counterparts at low redshifts, may be the signposts of massive elliptical galaxies, or clusters in the process of formation through a vigorous merger of smaller gas-rich galaxies (e.g., Djorgovski 1987). Prototypes of such systems are the radio galaxies 3C 326.1 (McCarthy et al. 1987) and 3C 294 (McCarthy et al. 1990b), both located near  $z = 1.8$ .

Major open questions concerning such objects include: (i) nature of the galaxy hosting the active nucleus, (ii) the dominant mechanism responsible for maintaining the ionization and the high degree of turbulence (or, velocity shear) in the Ly $\alpha$  cloud over several tens of kiloparsec, (iii) the geometry and the dynamic state of the cloud (infall, outflow, solid-body rotation). Here we report the discovery and extensive observations of an exceptionally interesting giant Ly $\alpha$  cloud associated with a powerful ultra-steep spectrum radio source at  $z = 2.468$ , which provides a new insight into the above issues.

## 2. Observations

The optical observations of the radio galaxy 0852+124 presented in this paper were carried out at ESO, La Silla, as part of an ongoing optical follow up of the Ooty sample of ultra-steep spectrum radio sources (Gopal-Krishna et al. 1992). The sample was mainly derived from the Ooty lunar occultation survey at 327 MHz for which radio spectral data were obtained with the 100-m Effelsberg Radio Telescope. The motivation for the optical follow up came from some early investigations of the 4C and the Ooty-occultation samples of radio sources, from which it was realized that sources with an ultra-steep spectrum

at decimetre wavelengths are likely to be more distant, on average (Tielens et al. 1979; Gopal-Krishna & Steppe 1981). This criterion has since proved to be very useful for discovering high- $z$  radio galaxies (e.g., Miley 1994 and references therein)

### 2.1. Radio observations

Details of the radio data will be presented in a separate paper (Kulkarni & Gopal-Krishna, in preparation). Here we only summarize the aspects directly relevant to the present discussion.

The Ooty occultation radio source OTL 0852+124 (List 9 : Joshi & Singal 1980) with a spectral index  $\alpha = -1.3$ , a flux density of about  $55 \text{ mJy}$  at 5 GHz, and lacking an optical counterpart on the Palomar-Sky-Survey prints belongs to the first set of objects which we selected for optical identification and spectroscopy. This was preceded by high-resolution imaging at 5 GHz with the VLA. The object is a classical double radio source with the two components separated by  $15''$  at position angle  $PA = 7^\circ$  (Fig. 3, see below). No radio core was detected between the components, down to  $0.5 \text{ mJy}$  level, which strongly suggests that the source is a radio galaxy. Coordinates (1950) of the mid-point between the two hotspots are :  $RA = 08^h 52^m 37.0^s$ ;  $Dec. = 12^\circ 28' 57''$ .

### 2.2. Broad-band optical imaging and low-resolution slit spectroscopy

A 10 minute V-band image of the field was obtained with EFOSC1 at the 3.6m telescope at La Silla on February 26, 1992 to search for the optical counterpart of the radio source. The detector used for this and all subsequent observations was a TEK512 CCD with a pixel size of  $0.61''$ . A finding chart made from that exposure is shown in Fig. 1. It reveals two objects near the radio source: a galaxy, labeled 'G', and a much fainter object labeled 'A'. Spectral data were obtained with the same instrument in January, 1993. Since the optical identification of the radio source was uncertain (object A being very faint, though lying closer to the radio center), the slit was oriented at a position angle of  $PA = -9^\circ$  and centered on the galaxy G so as to cover the faint object A as well. Three 50-minute spectra were obtained using the grism B300 that yields a spectral coverage from  $3640 \text{ \AA}$  to  $6860 \text{ \AA}$  at  $6 \text{ \AA}$  per pixel corresponding to a spectral resolution of  $\sim 20 \text{ \AA}$  for the  $2''$  slit.

On the sky-subtracted median of the three exposures the object G shows an emission line at  $\lambda = 6352 \text{ \AA}$  which we identify with  $[OIII]\lambda 3727$  at  $z = 0.704$ . This identification is supported by a clear break seen in the rest-frame continuum near  $4000 \text{ \AA}$ . More interestingly, the spectrum of the region near the object A (Fig. 2) shows a strong, very extended (overall  $\sim 9''$ ), and resolved ( $FWHM \approx 35 \text{ \AA}$ ) emission line at  $4217 \text{ \AA}$ , with an enormous equivalent width ( $EW \sim 3500 \text{ \AA}$ ) and a tilt corresponding to a maximum velocity field of  $\approx 1100 \text{ km s}^{-1}$ . Since these properties are hallmarks of Ly $\alpha$  radio galaxies, we identified the intense line as Ly $\alpha$  at  $z = 2.468 \pm 0.001$ .

As indicated by the large equivalent width of the line, the continuum is extremely weak in the region of the extended Ly $\alpha$

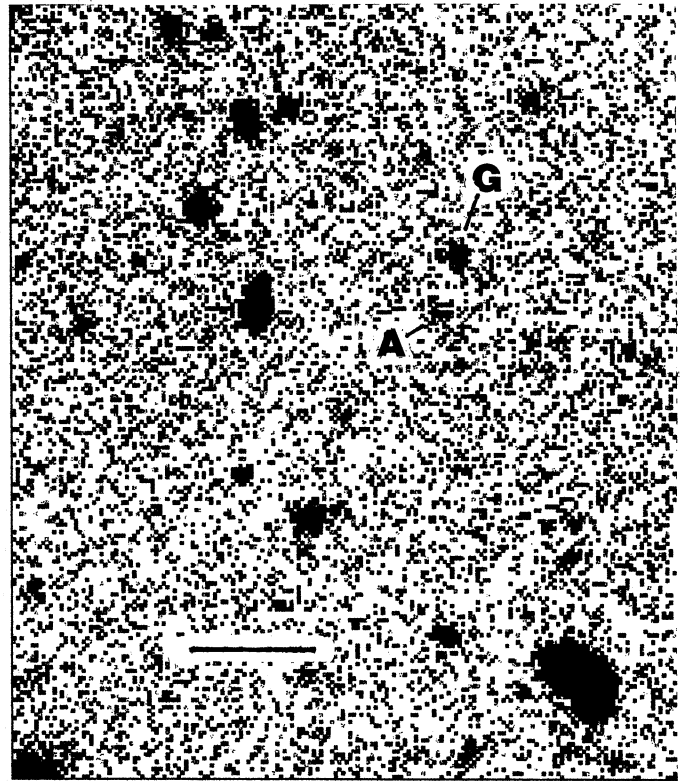
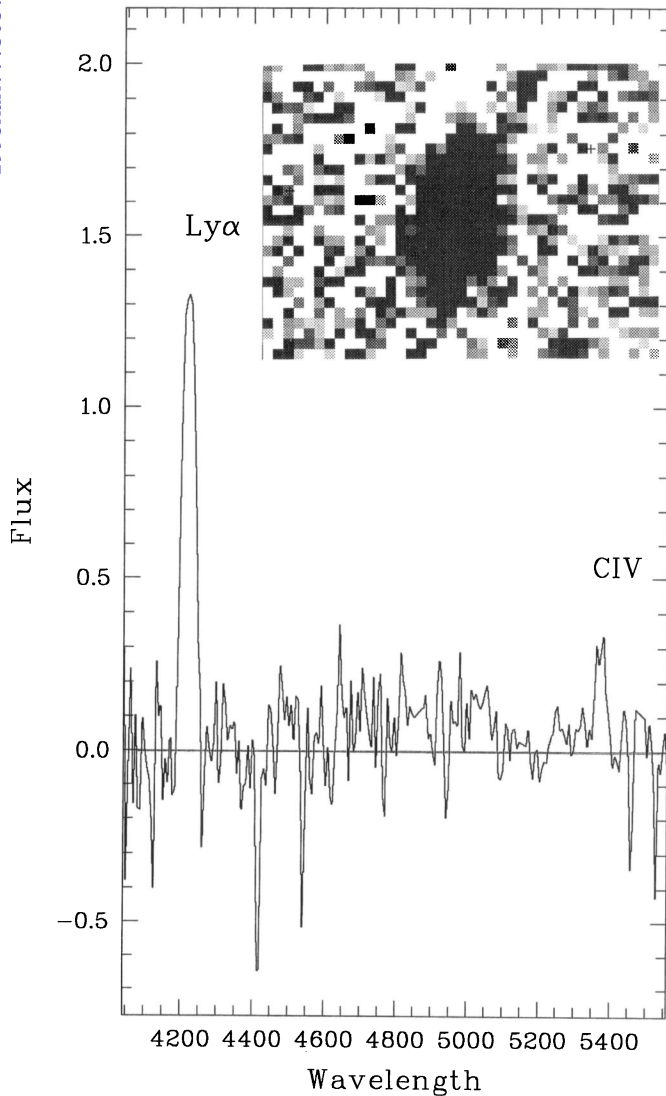


Fig. 1. A finding chart made from a V-band exposure of the field of 0852+124. Galaxy G and object A are indicated. A is the parent galaxy of the radio source and lies at the northern edge of the Ly $\alpha$  cloud. North is up, East is to the left. The bar measures  $20''$

line. There is, however, a hint of continuum at redder wavelengths which appears stronger in the northern part of the cloud (cf. Figs. 2 and 3). We think that this continuum may be real because it almost coincides with the position of object A in the broad-band V image (Fig. 1). There are no features in the continuum except for the Ly $\alpha$  line and a very faint patch at  $\lambda = 5373 \text{ \AA}$  which is spatially much less extended than Ly $\alpha$  and is localized near object A. It can be identified as CIV at  $z = 2.469$ . Its redshift coincidence with Ly $\alpha$ , and the large width ( $FWHM \approx 30 \text{ \AA}$ ) implying that the signal extends over a few pixels, suggest that the faint feature may be real. If so, the ratio of intensities in the region where CIV is detected is  $CIV/Ly\alpha = 0.25 \pm 0.1$ . Apparent magnitudes of the two galaxies, determined using Landolt (1992) standard stars are:  $m_V = 21.7 \pm 0.1$  (G), and  $m_V = 23.3 \pm 0.4$  (A).

### 2.3: Narrow-band optical imaging and intermediate resolution slit-spectroscopy

Three narrow-band images of 1800 s, 3000 s and 3600 s integrations were obtained with EFOSC1 on March 4, 1994 using a combination of 3 filters (two in the filter wheel and one in the grism wheel) that yielded a peak transmission of 50 % centered at  $4200 \text{ \AA}$  with a half-width of  $\approx 100 \text{ \AA}$  and no red leak. The sky conditions were non-photometric and the seeing was



**Fig. 2.** A 4-pixel wide extraction made from the low-dispersion spectrum, at the location of the [CIV]1549 line. The vertical scale is in arbitrary units. The inset showing the clearly tilted Ly $\alpha$  line covers a total velocity field of  $15000 \text{ km s}^{-1}$  along the horizontal axis and a total spatial extent of  $15''$  along the vertical axis (north is up)

$1.5''$ . The three frames were registered to sub-pixel precision and co-added. The resulting image (the Ly $\alpha$  cloud) is shown in Fig. 3.

Intermediate-resolution spectra of the extended Ly $\alpha$  cloud were obtained on the nights of March, 16, 17 and 18, 1994 (one spectrum per night) under variable conditions with an average seeing of  $1.5''$ . We used the B150 grism and a  $1.5''$  slit which give a resolution of  $8 \text{ \AA}$ . The slit was (blindly) positioned at the centre of the narrow-band image. Two spectra were acquired near the position angle of the radio source ( $PA = 10^\circ$ ), and one in the east-west direction (i.e., roughly perpendicular to the radio PA at  $7^\circ$ ). The exposure times were  $5400 \text{ s}$  and  $7200 \text{ s}$  at  $PA = 10^\circ$  and  $6600 \text{ s}$  at  $PA = 90^\circ$ . The spectra were flux-calibrated using the standard star LTT6248 observed at an airmass very

close to unity. The only feature visible in these spectra is Ly $\alpha$ . No continuum was detected (Fig. 4). The non-detection of the CIV feature in these spectra does not necessarily rule out the reality of the line in the low resolution data. The combination of higher spectral resolution and cirrus during the 5200s exposure, lowers the effective exposure time of the relevant ( $PA=10^\circ$ ) data to less than 2 hours.

#### 2.4. Astrometry

In order to overlay the optical and radio images of the source, we measured positions of six stars (secondary calibrators) in the EFOSC field, to  $1.5''$  accuracy relative to a grid of six SAO stars using the Palomar-Sky-Survey prints. The primary astrometric solutions were accurate to  $\pm 0.5''$  in each coordinate and the derived final positions of the objects on the EFOSC1 frames are accurate to  $< 1''$ . We used the secondary calibrators to determine the position angle and the scale of the EFOSC1 frames using only the linear terms in the solution. Figure 3 shows the radio contours superimposed on the narrow-band image of the Ly $\alpha$  cloud. Ignoring systematic errors due to possible differences in the radio and optical reference frames we estimate the registration to be accurate to  $\pm 1''$ .

### 3. Results

The overall extent of the Ly $\alpha$  cloud is  $\sim 9''$ . The Ly $\alpha$  flux integrated along the slit at  $PA = 10^\circ$  is  $13 \times 10^{-16} \text{ ergs}^{-1} \text{ cm}^{-2}$ , and at  $PA = 90^\circ$  it is  $9 \times 10^{-16} \text{ ergs}^{-1} \text{ cm}^{-2}$ . From this and the measured size of the cloud, we estimate its integrated Ly $\alpha$  flux to be around  $50 \times 10^{-16} \text{ ergs}^{-1} \text{ cm}^{-2}$ . For an assumed cosmology with  $H_0 = 75 \text{ h km s}^{-1} \text{ Mpc}^{-1}$  and  $q_0 = 0$ , the measured redshift of  $z = 2.468$  corresponds to a spatial scale of  $1'' = 8.9 \text{ h}^{-1} \text{ kpc}$ , implying overall sizes of  $134 \text{ h}^{-1} \text{ kpc}$  and  $\sim 80 \text{ h}^{-1} \text{ kpc}$ , respectively, for the radio source and the Ly $\alpha$  cloud. The integrated radio and Ly $\alpha$  luminosities are  $\simeq 5 \times 10^{45} \text{ h}^{-2} \text{ ergs}^{-1}$  and  $\approx 3 \times 10^{44} \text{ h}^{-2} \text{ ergs}^{-1}$ , respectively. We now proceed to discuss the nature of the Ly $\alpha$  cloud and its likely relationship with the radio source.

#### 3.1. The Ly $\alpha$ morphology

Figure 3 displays the Ly $\alpha$  cloud at two different contrasts. Despite the prevailing moderate seeing conditions, a *highly uneven* brightness distribution is clearly visible consisting of several clumps and filaments spread across most of the space between the radio centre, which lies within  $1''$  of the position of object A, and the southern radio hot spot (Fig. 3a). The Ly $\alpha$  cloud is distinctly offset from the hot spot towards the parent galaxy (object A). At lower contrast the bright inner ridge of the cloud is found to be extended along the radio axis. The faint patch of optical emission at the southern edge of the hot spot is most probably real and is likely to be associated with the bow shock of the advancing radio lobe. This patch is detected at the  $3-4 \sigma$  level and has a Ly $\alpha$  luminosity of  $\sim 2 \times 10^{43} \text{ h}^{-2} \text{ erg s}^{-1}$ .

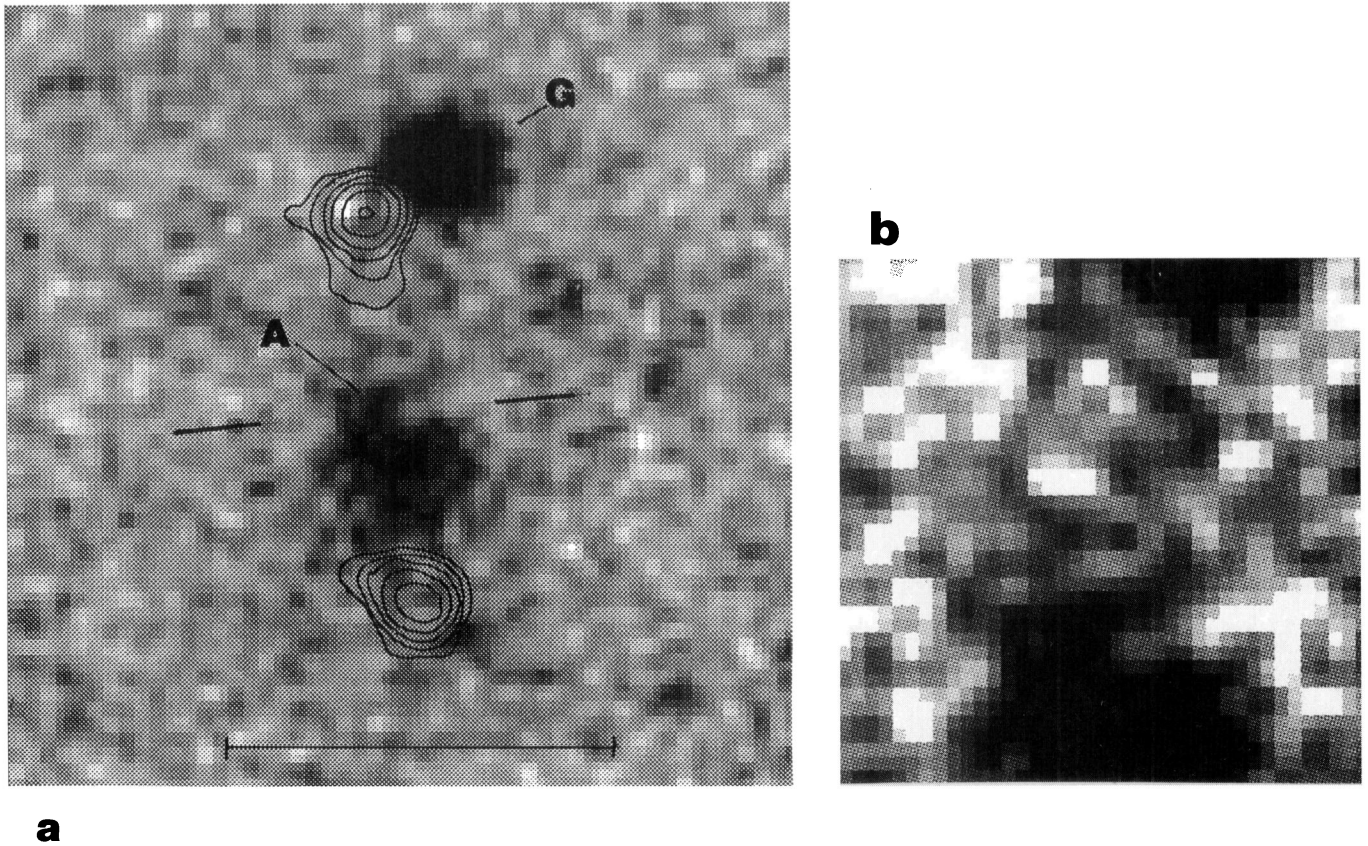


**Fig. 3.** **a** Narrow-band image of the object, taken with a filter of half-width  $\approx 100 \text{ \AA}$  centered at the Ly $\alpha$  line. North is up, East is to the left. The bar near the lower boundary measures  $15''$ . The giant Ly $\alpha$  cloud is seen near the central region. The other bright object to the north is the foreground galaxy 'G' unrelated to the cloud and the radio source. The object 'A' is identified as the parent galaxy of the double radio source whose radio contours at 5 GHz are overlaid on the associated Ly $\alpha$  cloud. The beamwidth of the radio map is  $1.5''$  and the contour levels are: 0.5, 1, 2, 4, 8 and 16 mJy/beam. The patchy structure of the Ly $\alpha$  nebula can be noticed. The nebula appears highly asymmetric relative to the radio emission, being seen essentially in the southern half of the radio source. The faint optical patch seen at the outer edge of the southern radio hot spot is significant and is likely to mark the location of the bow-shock. The thick lines point at the narrow regions of depressed Ly $\alpha$  emission on either side of the 'neck' (object A), which are reminiscent of dust lanes observed in nearby radio galaxies. **b** The 'dust-lanes' seen at a higher contrast (The abrupt fall in Ly $\alpha$  intensity to the north of the neck is graphically illustrated in Fig. 5 and is interpreted as being the result of obscuration by the dusty disk (Sect. 4)

The morphology of the northern part of the Ly $\alpha$  cloud is specially interesting (Fig. 3). There is a faint feature, shaped like an arc (akin to a bull's horns). Immediately to the south of the horns lies a narrow spot of emission (the 'neck') which is spatially coincident with galaxy A (Fig. 3a). We identify it with the radio source as it lies within  $1''$  of the mid-point between the two radio hot spots. The conspicuous lack of emission to the east and west of the neck (indicated by a pair of thick lines in Fig. 3a) is reminiscent of *dust-lanes* observed in many nearby radio galaxies. The abrupt cut-off in Ly $\alpha$  brightness to the north of the neck, forming a 'straight edge' of fading emission, is consistent with the idea that the neck is physically associated with an obscuring east-west disk of dust (Figs. 3 & 5). Further,

the postulated disk is seen to be almost precisely perpendicular to the radio source axis, which conforms entirely to the well known behaviour of the dust-lanes found in nearby radio galaxies (Kotanyi & Ekers 1979; Mollenhoff et al. 1992).

### 3.2. The velocity field

The most striking feature of the slit-spectra shown in Fig. 4 is that *in both position angles the Ly $\alpha$  emission is split into two main velocity components*. The intrinsic widths (FWHM) as well as the separation of the components are of order  $\approx 1100 \text{ km s}^{-1}$ . We think that the line-splitting in velocity space is primarily due to bulk motion of the gas, although we cannot exclude radiative transfer effects (e.g. Chen & Neufeld 1994).

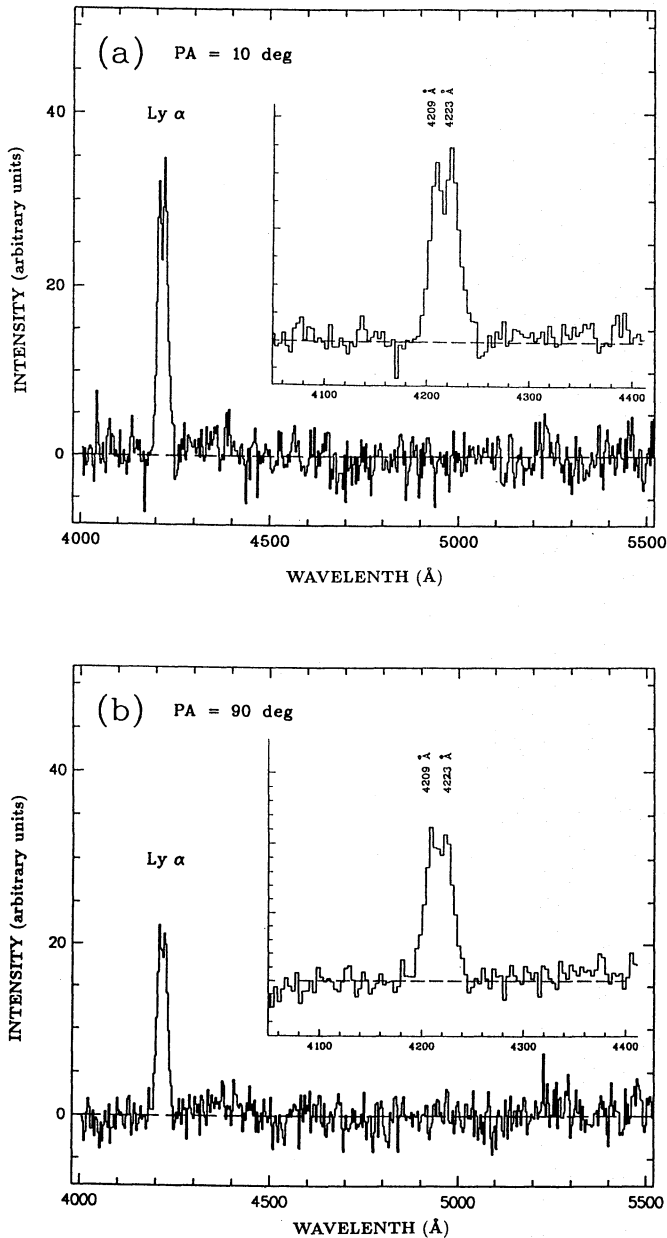


**Fig. 4.** **a** Medium resolution spectrum (integrated along the slit) obtained with a slit oriented at  $PA = 10^\circ$  (i.e. close to the radio axis) showing that the Ly $\alpha$  line is split into two components. No continuum is detected. The inset shows an enlargement of the Ly $\alpha$  profile. **b** Same as in **a**, but for the slit oriented at  $PA = 90^\circ$ . The line-splitting is less evident on the 1-D spectrum taken at  $PA = 90^\circ$  because the velocity difference varies from  $\sim 200 \text{ km s}^{-1}$  to  $\sim 1100 \text{ km s}^{-1}$  along the slit as seen on the 'phase-space' diagram in Fig. 6

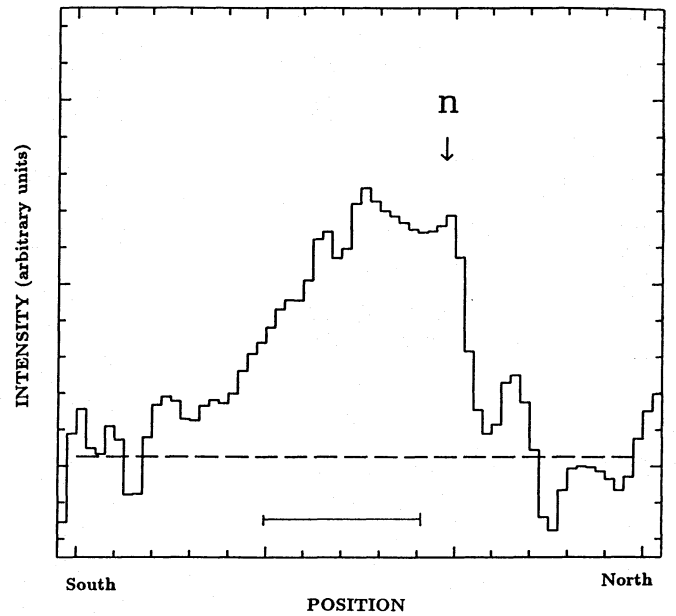


**Fig. 5.** A North-South luminosity profile of the Ly $\alpha$  cloud obtained by averaging 3 columns ( $1.8''$ ) centered at the position of the 'neck' (marked by 'n' on the figure). North is to the right. The profile shows a smooth decline to the south, but an abrupt fall to the north, which we interpret as being due to dust obscuration. The bar measures  $5''$

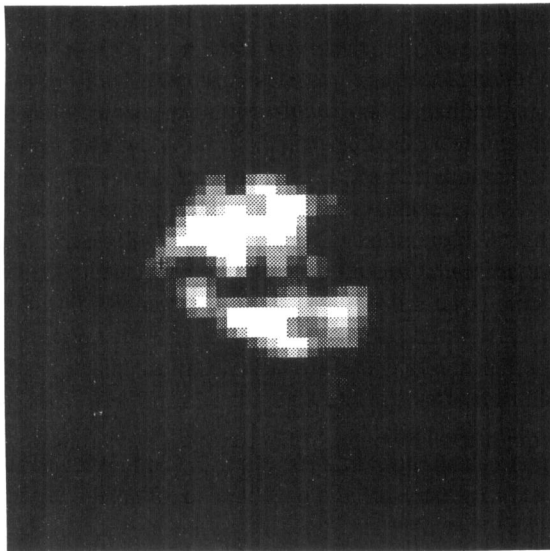
Another important feature of the spectra is that, at a given velocity, the line emission is concentrated into clumps thus confirming the impression one gets from the unevenness of the narrow-band image. This is readily evident from Fig. 6, which shows the 'phase-space' diagrams derived from the slit-spectra taken nearly along ( $PA = 10^\circ$ ) and perpendicular ( $PA = 90^\circ$ ) to the radio axis.

The overall spatial extent of the line seen in the spectrum obtained at  $PA = 90^\circ$  is  $\approx 8''$  (Fig. 6a), which corresponds to  $70 h^{-1} \text{ kpc}$ . The peak-to-peak velocity difference between the two velocity components varies from  $\sim 200 \text{ km s}^{-1}$  to  $\sim 1100 \text{ km s}^{-1}$  in the rest frame. At  $PA = 10^\circ$  (Fig. 6b), the maximum spatial extent of the nebula is  $9''$  ( $80 h^{-1} \text{ kpc}$ ) and the two main components are separated by  $\sim 1100 \text{ km s}^{-1}$ . The lower redshift component consists of two clumps.

### 3.3. Ionization of the Ly $\alpha$ cloud

With just one well-detected line it would be premature to attempt a quantitative assessment of the ionization mechanism. However, the probable detection of CIV emission near the inferred location of the nucleus (object A) with an intensity of  $\sim 25\%$  of Ly $\alpha$  favours the AGN as the main source of ionizing photons for the region of the neck (see, Ferland & Osterbrock 1986). The AGN emission in our direction is probably blocked almost totally by the dust-lane (Sect. 3.1), or a by dusty nuclear torus (e.g., Antonucci 1993).

Another potential source of ionizing photons is star-formation triggered by the jets/hotspots (Rees 1989; Begelman & Cioffi 1989; De Young 1989), for which recent evidence has



(a)

10''

(b)

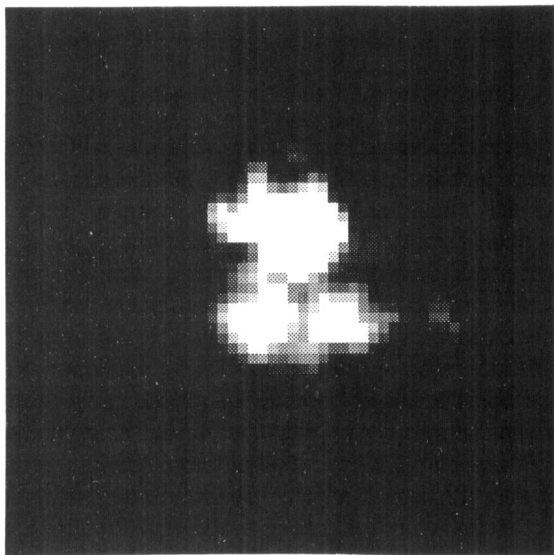


**Fig. 6.** **a** ‘Phase-space’ diagram obtained from the slit-spectrum oriented at  $PA = 90^\circ$ , i.e. roughly perpendicular to the radio axis. The horizontal axis displays the spatial scale, with east increasing to the right. The vertical axis covers a total velocity field of  $7000 \text{ km s}^{-1}$ . Two distinct velocity components are visible. The velocity splitting decreasing from the center to the edge is characteristic of nebula undergoing lateral expansion or contraction. **b** Same as in **a** but for the slit oriented at  $PA = 10^\circ$ . South increases to the right. Again, two velocity components are seen; the one at lower velocity is resolved into two clumps. Both these diagrams are interpreted in terms of a roughly cylindrical shell made of clumps of ionized gas expanding perpendicularly to the radio axis ( $PA = 7^\circ$ )

come from the HST imaging of the high- $z$  radio galaxy 4C41.17 (Miley et al. 1992). In our case, however, the observed Ly $\alpha$  equivalent-width of about  $1000 \text{ \AA}$  in the rest-frame is too large to favour the possibility of massive stars being the source of ionization (see, Meier 1976; Chambers & McCarthy 1990).

An important source of energy input to the Ly $\alpha$  cloud could be the bow-shock associated with the southern radio lobe (see below). Detailed studies of nearby radio galaxies have provided evidence for such an interaction which can excite the ambient gas and establish large-amplitude velocity fields well in excess of the escape velocity (e.g., van Breugel et al. 1986; Danziger & Focardi 1988). Considering that we do not detect CIV near the peak of Ly $\alpha$  down to 2% of Ly $\alpha$ , collisional excitation by the bow-shock, or photoionization by X-rays produced in the tenuous medium heated by the bow-shock remain a viable option for the ionization of the cloud (see, e.g., Baum & Heckman 1989; Sutherland et al. 1993). Assuming 10% efficiency for radio emission the kinetic power of the (southern) bow-shock would be  $\sim 3 \times 10^{46} \text{ erg s}^{-1}$ , almost 2 orders-of-magnitude higher than the observed Ly $\alpha$  output of the cloud. This ratio is consistent with the relation found between the jet power and the extended narrow-line emission of powerful radio galaxies (Rawlings & Saunders 1991).

#### 4. Discussion

##### 4.1. Possible origin of the Ly $\alpha$ asymmetry

The morphology and the phase-space structure of the Ly $\alpha$  cloud, as well as its positional offset from the radio nucleus lead us to the following picture. The neck is located at the nucleus of the double radio source which coincides with galaxy A. The galaxy is encircled by an extended disk of dust which is almost precisely perpendicular to the radio axis and, hence, probably related to the collimation of the radio jets. The main body of the parent galaxy is significantly occulted by the disk since at  $z = 2.468$  we are observing UV emission. Due to obscuration by the dusty disk, we only see the part of the Ly $\alpha$  cloud which is on the near side of the radio nucleus. Discounting the unlikely possibility that the disk is totally planar and is viewed precisely edge-on, any part of the Ly $\alpha$  cloud on the far side of the nucleus would be efficiently obscured by the dusty disk.

An important consistency check on this scenario comes from the observed systematic velocity gradient of  $\sim 1100 \text{ km s}^{-1}$  of the Ly $\alpha$  cloud along the radio axis, as estimated from the low-dispersion slit spectrum (Fig. 2). In our picture, further justified below, the region south of the nucleus where the cloud is observed is the near side of the radio source. The gaseous medium (and the embedded Ly $\alpha$  filaments) closer to the centre/dust-lane would have a relatively tight dynamic coupling to the parent galaxy. In contrast, the medium far away from the galaxy, being more tenuous, would be accelerated outward more effectively (and more recently) by the bow-shock of the outflowing radio plasma. Consequently, the part of the Ly $\alpha$  cloud closer to us would be expected to approach us at a faster rate than the part closer to the main body of the galaxy. Such a dynamical pat-

tern is, in fact, consistent with the sense of the tilt observed in the low-resolution spectrum taken with a north-south slit (i.e., nearly along the radio axis). It shows clearly that *the southern part of the cloud is approaching towards us at a rate of  $\sim 1100 \text{ km s}^{-1}$* , relative to its northern part (Fig. 2). This lends credence to our assumption that the southern radio lobe is the one approaching us and, hence, lies on the near side of the active nucleus.

#### 4.2. Comparison with other giant Ly $\alpha$ clouds

The trend for Ly $\alpha$  emission to appear brighter on the side of the *nearer* radio lobe (the approaching one) is *also* evident in cases of other high- $z$  radio galaxies where the Ly $\alpha$  brightness shows a similar distinct asymmetry about the nucleus *and* the approaching radio lobe can be identified (by an observed decrease in redshift from the nucleus towards the outer edge of the lobe). These high- $z$  radio galaxies are: 3C 294 ( $z = 1.82$ ; McCarthy et al. 1990b), 4C 41.17 ( $z = 3.8$ ; Chambers et al. 1990) and 8C 1435+635 ( $z = 4.25$ ; Lacy et al. 1994; Spinrad et al. 1995.). We propose that the Ly $\alpha$  asymmetry in all these systems can also be due to a giant obscuring disk of dust. Indeed, the presence of such a disk can be inferred in all these sources from the steep gradient observed in the Ly $\alpha$  brightness near the nucleus and stretched normal to the radio axis. In fact, Dunlop et al. (1994) have recently identified a narrow band of depressed Ly $\alpha$  brightness in 4C 41.17, coincident with the radio nucleus and extended normal to the radio axis, which they interpret as the dusty disk responsible for the submillimetre emission detected by them (also, Chini & Krugel 1994). A similar band of depressed intensity is found across the bright and highly extended ( $\sim 110 \text{ kpc}$ ) Ly $\alpha$  nebula associated with the radio galaxy 2104-242 ( $z = 2.49$ ) (see, McCarthy et al. 1990a). In another two high- $z$  radio galaxies, namely, 3C 326.1 ( $z = 1.82$ ) and 6C 1232+39 ( $z = 3.22$ ), the associated Ly $\alpha$  emission is likewise very extended, bright, and highly asymmetric about the nucleus, being much brighter on the western side in each case (McCarthy et al. 1987; Eales et al. 1993). If our model is true in general, we expect that the recession velocity near the western edge of the cloud would be found to be smaller compared to that near the nucleus.

#### 4.3. Radio lobe driven expansion of the Ly $\alpha$ cloud

Although broad Ly $\alpha$  profiles ( $FWHM \geq 1000 \text{ km s}^{-1}$ ) are well known attributes of giant Ly $\alpha$  clouds in distant radio galaxies, the slit-spectroscopy of our cloud at both position angles has revealed a new feature: *the line is clearly split*, by about  $\Delta V \approx 1100 \text{ km s}^{-1}$  at most locations across the cloud. The line-splitting is highly reminiscent of the nearby radio galaxy 3C 120 where the slit-spectrum taken along the radio jet shows a clear splitting of the [OIII] lines by  $\sim 300 \text{ km s}^{-1}$  along the inner 5 kpc of the jet (Axon et al. 1989). These authors convincingly interpreted the spectra in terms of a cylindrical *cocoon* of line-emitting plasma, which surrounds the jet and was set into lateral expansion by it (see, also, Akujor & Jackson

1992). Most probably, then, our Ly $\alpha$  cloud, too, is undergoing a *lateral expansion*, driven by the radio lobe which it presumably surrounds. Although the postulated radio lobe at the position of the cloud is not apparent on our high-resolution radio map, it is almost certainly present and should show up on maps more sensitive to diffuse emission as found to be the case for powerful radio sources when imaged with a high dynamic range (see, e.g., Leahy et al. 1989; Bridle et al. 1994).

The proposal that the Ly $\alpha$  cloud is a giant expanding cocoon of thermal plasma surrounding the (roughly cylindrical) radio lobe is further strengthened by the observed shape of the phase-space diagram obtained with the slit positioned normal to the lobe axis. The slit samples a thin (annular) *slice* of the cloud perpendicular to its proposed symmetry axis (Fig. 6a). Consistent with the proposed geometry of expansion, the velocity-splitting is found to almost vanish near the western edge of the slice; near the eastern edge the line-emitting material is too deficient and hence the observed emission too faint to reveal the kinematic pattern in that region with any degree of certainty. An estimate of the ‘diameter’ ( $2r$ ) of the postulated inner void of the cloud (which, in our scheme, would approximately correspond to the width of the radio lobe) comes from the spatial scale of the central depression observed in the phase-space diagram (Fig. 6a), which amounts to  $\approx 3''$ , i.e.  $27 h^{-1} \text{ kpc}$ .

## 5. Deductions and conclusions

### 5.1. Phenomenology

To sum up, our picture for this remarkable object is that the ejection of radio jets, probably triggered by the accretion of dusty material onto a collapsed object blew an expanding radio cavity through a pre-existing giant circum-galactic nebula (cf., Scheuer 1974; Carilli et al. 1994) with a two-phase temperature/density structure (Rees 1988). This created a cocoon of nebular gas around the cavity compressed, heated, and accelerated from within by the expanding radio lobe(s) and the bow-shock(s). Denser clumps in this ionized cocoon manifest as the Ly $\alpha$  cloud (a similar scenario has been proposed by Meisenheimer & Hippelein 1992, to explain the extended [OII] $\lambda 3727$  emission around the radio galaxy 3C 368). In the present case, the visibility of the Ly $\alpha$  cloud would be further enhanced due to the high turbulence generated through interaction with the radio lobe, which is expected to raise the escape probability of the Ly $\alpha$  photons against resonant trapping within the nebula (where a small amount of dust may well be present). The proposed role of the radio lobe in the creation and visibility enhancement of the Ly $\alpha$  complex is supported by the finding of Heckman et al. (1991) who noticed a lack of spatially-resolved Ly $\alpha$  nebulosities among radio quasars with under-developed radio lobes (i.e.,  $\leq 10 \text{ kpc}$ ).

### 5.2. Energetics and the time scale of radio activity

Schematically then, the present Ly $\alpha$  complex can be perceived to be a giant cylindrical shell of clumped thermal plasma, oriented along the radio axis and undergoing a lateral expansion at

a rate of  $V_e \approx 550 \text{ km s}^{-1}$ . Following McCarthy et al. (1990b) and Heckman et al. (1991), we estimate the total mass of the cloud to be  $\sim 4.10^7 M_\odot$ , taking a diameter of  $6''$  for the main body of the cloud and assuming case B recombination together with a filling factor of order  $10^{-7}$ . The mass estimate has a very large uncertainty due to the unknown ionization mechanism and filling factor but allows us to obtain a rough estimate of the kinetic power of bulk expansion ( $\sim 2.10^{56} \text{ erg}$ ) which is only a tiny fraction of the estimated power ( $\approx 2.10^{61}$ ) injected by the jet over the lifetime of the radio source (see below). Thus, even if our mass estimate is off by orders of magnitude, the proposed radio lobe driven expansion of the Ly $\alpha$  cloud would still remain energetically feasible.

A very useful quantity that can be inferred from the estimated bulk expansion velocity is the dynamical time-scale for the formation of the line-splitting region ( $r/V_e \approx 2 \cdot 10^7 \text{ h}^{-1} \text{ yr}$ ). This is a rather direct measure of the age of the radio source, which concurs with typical estimates obtained for radio galaxies employing other methods, such as by measuring the gradient of radio spectral index along the lobe (e.g., Alexander & Leahy 1987; Fey et al. 1986), or from beam-propagation models of double radio sources (eg. Gopal-Krishna & Wiita 1991).

### 5.3. The dynamical pattern

The foregoing discussion argues for association of huge dusty disks with high- $z$  radio galaxies, including those which are sometimes termed “pure hydrogen nebulae” implying little dust content. Such dusty disks can be inferred from the observed asymmetry (about the active nucleus) and sharp gradients in the extended Ly $\alpha$  distribution, supplemented by velocity-field measurements. The proposed scenario, thus, allows us to predict the sense of velocity gradients across some prominent examples of high- $z$  radio galaxies showing a distinctly asymmetric Ly $\alpha$  brightness distribution (e.g., 3C 326.1 and 6C 1232+39; Sect 4.2). Also, one would expect that the slit spectrum taken perpendicular to the radio lobe axis would yield a phase-space diagram with signatures of an expanding cocoon (Fig. 6a).

### 5.4. Dust in high- $z$ radio galaxies

The extended Ly $\alpha$  emission associated with radio galaxies, probably provoked and enhanced by their radio lobes, provides a unique diagnostic for dust in such extremely distant objects. The presence of dusty disks can, however, significantly depress the optical flux from their parent galaxies (which was emitted in the UV), thereby making their detection difficult and, moreover, complicating the interpretation of their spectra.

The prevalence of dusty disks in distant radio galaxies, as surmised here appears to have a close relevance to the properties of the giant ( $\sim 100 \text{ kpc}$ ) Ly $\alpha$  nebulae detected by Heckman et al. (1991) around several radio-loud quasars. Clearly, in the case of quasars, structural details of the associated Ly $\alpha$  nebulae are much harder to decipher, e.g., due to the presence of the intense nuclear Ly $\alpha$  emission. Nonetheless, these authors

have noticed a fairly distinct trend for the Ly $\alpha$  nebulosity to be brighter on the side of stronger radio emission. Aside from invoking an intrinsically asymmetric Ly $\alpha$  emission as an explanation, they have also considered the possibility that the nebulae are intrinsically symmetric, but appear asymmetric due to the integrated dust extinction being less for the near side of the radio source (where the radio emission would appear stronger due to relativistic Doppler boosting). This latter alternative would be in accord with the evidence for dusty disks presented here. Indeed, beginning with the classical example of the nearest radio galaxy, Cen A, the ‘dusty disk - radio galaxy’ connection appears to pervade all the way up to the highest redshifts where radio galaxies are known to exist.

### References

- Akujor, C. E., Jackson, N., 1992, AJ, 104, 546.  
 Alexander, P., Leahy, J. P., 1987, MNRAS, 225, 1.  
 Antonucci, R., 1993, ARA&A, 31, 473.  
 Axon D. J., Unger, S.W., Pedlar, A., Meurs, E. J., Whittle, D.M., Ward, M.J., 1989, Nature, 341, 631.  
 Baum, S. A., Heckman, T. M., 1989, ApJ, 336, 681.  
 Begelman, M. C., Cioffi, D. F., 1989, ApJ, 345, L21.  
 Bridle, A.H., Hough, D. H., Lonsdale, C. J., Burns, J. O., Laing, R. A., 1994, AJ, 108, 766.  
 Carilli, C. L., Perley, R. A., Dreher, J. H., 1988, ApJ, 334, L73.  
 Carilli, C. L., Perley, R. A., Harris, D. E., 1994, MNRAS, 270, 173.  
 Chambers, K. C., McCarthy, P. J., 1990, ApJ, 354, L9.  
 Chambers, K. C., Miley, G. K., van Breugel, W. J. M., 1990, ApJ, 363, 21.  
 Chen, W.L., Neufeld, D., 1994, ApJ, 432, 567.  
 Chini, R., Krugel, E., 1994, AA, 288, L33.  
 Danziger, I. J., Focardi, P., 1988, in: “Cooling flows in clusters and galaxies”, Kluwer, A. C. Fabian (ed), p.133.  
 De Young, D.S., 1989, ApJ, 342, L59.  
 Djorgovski, S., 1987, in: “Starburst and galaxy evolution”, Edition Frontiers, T. X. Thuan, T. Montmerle & T. Thanh van, p. 549.  
 Dunlop, J.S., Hughes, D.H., Rawlings, S., Eales, S.A., Ward, M.J., 1994, Nature, 370, 347.  
 Eales, S.A., Rawlings, S., Dickinson, M., Spinrad, H., Hill, G.J., Lacy, M., 1993, ApJ, 409, 578.  
 Ferland, G. J., Osterbrock, D. E., 1986, ApJ, 300, 658.  
 Fey, A. L., Spangler, S. R., Myers, S. T., 1986, AJ, 91, 1279.  
 Gopal-Krishna, Melnick, J., Giraud, E., Steppe, H., 1992, AA, 254, 42.  
 Gopal-Krishna, Steppe, H., 1981, AA, 101, 315.  
 Gopal-Krishna, Wiita, P.J., 1991, ApJ, 373, 325.  
 Heckman, T. M., Lehnert, M. D., van Breugel, W., Miley, G. K., 1991, ApJ, 370, 78.  
 Heckman, T. M., van Breugel, W. J. M., Miley, G.K., 1984, ApJ, 286, 509.  
 Joshi, M.N., Singal, A.K., 1980, Bull. Astron. Soc. India, 1, 49.  
 Kotanyi, C. G., Ekers, R.D., 1979, AA, 73, L1.  
 Lacy, M. et al., 1994, MNRAS, 271, 504.  
 Landolt, A. U., 1992, AJ, 104, 340.  
 Leahy, P.J., Muxlow, T. W. B., Stephens, P. W., 1989, MNRAS, 239, 401.  
 McCarthy, P. J., Kapahi, V. K., van Breugel, W., Subrahmanya, C. R., 1990a, AJ, 100, 1014.  
 McCarthy, P. J., Spinrad, H., Djorgovski, S., Strauss, M.A., van Breugel, W., Liebert, J., 1987, ApJL, 319, L39.



- 1995A&A...303..705G
- McCarthy, P.J., Spinrad, H., van Breugel, W., Liebert, J., Dickinson, M., Eisenhardt, P., 1990, ApJ, 365, 487.
- Meier, D. L., 1976, ApJ, 207, 343.
- Meisenheimer, K., Hippelein, H., 1992, AA, 264, 455.
- Miley, G.K., in: "The Physics of active galaxies", ASP Conf. Series, G.V. Bicknell, M. A. Dopita & P. J. Quinn (eds), p.385.
- Miley, G.K., Chambers, K.C., van Breugel, W., Machetto, F., 1992, ApJ, 401, L69.
- Mollenhoff, C., Hummel, E., Bender, R., 1992, AA, 255, 35.
- Pedlar, A., Dyson, J. E., Unger, S. W., 1985, MNRAS, 214, 463.
- Rawlings, S.A., Saunders, R., 1991, Nature, 349, 138.
- Rees, M. J., 1988, MNRAS, 231, 91P.
- Rees, M., 1989, MNRAS, 239, 1P.
- Scheuer, P.A.G., 1974, MNRAS, 166, 513.
- Spinrad, H., 1987, in: "High redshift and primeval galaxies", Edition Frontieres, J. Bergeron et al. (eds), p.59.
- Spinrad, H., 1989: in " The epoch of galaxy formation", Kluwer, S. Frenk et al. (eds), p39.
- Spinrad, H., Dey, A., Graham, J.R., 1995, ApJ, 438, L51.
- Sutherland, R. S., Bicknell, G. V., Dopita, A., 1993, ApJ, 414, 510.
- Tielens, A. G., Miley, G. K., Willis, A., 1979, AAS, 35, 153.
- van Breugel, W. J. M., Heckman, T. M., Miley, G. K., Filippenko, A. V., 1986, ApJ, 311, 58.
- Wilson, A.S., 1989, in: " Extranuclear activity in galaxies", ESO Workshop, E. J. A. Meurs & R. A. E. Fosbury (eds), p. 215.

This article was processed by the author using Springer-Verlag L<sup>A</sup>T<sub>E</sub>X A&A style file version 3.